Influence of the wettability nature of the nozzle wall on the dynamics of drop formation

Pardeep Bishnoi[*], Mrityunjay K. Sinha

Department of Mechanical Engineering, National Institute of Technology, Jamshedpur 831013, India

Corresponding Author Email: mail2pardeepbishnoi@gmail.com

ABSTRACT

This paper describes the Volume of Fluid model in which a driving force is applied to stimulate the droplet ejection. Through this model, the wettability of the nozzle's inner wall will be determined as it plays a vital role in the droplet's shape and size. The effect of parameters viz. breakup thread length, breakup velocity, breakup/ detachment time on the drop formation are computed in this paper by using volume of fluid method. The results indicate that the increase in contact angle of the nozzle inner wall reduces the drop's breakup time while increasing the breakup velocity and thread length of the drop. Also, the results indicate the reduction in quality of drop formation with increased hydrophobic nature, which is not suitable for spray painting or in inkjet printing. Similarly, the deterioration in the quality of drop formation is due the more hydrophilic nature of the nozzle.

1. INTRODUCTION

In the last few years, a lot of work has been done on the drop formation process, but the basic principle of the drop dynamics process remained the same. Use of droplets in industrial processes has been increased tremendously. In the current era, almost every sector like automobile painting, inkjet printing, fuel injection, medicine and agricultural sector implements the droplet generation as per their requirements [1-5]. In all, these applications have to deal with high speed and high accuracy during drop formation process. Eggers [6] reviewed the process of drop formation in a thorough manner starting from drop's formation to its detachment into primary and secondary droplets. Recent advancements in the technical field allow high-speed cameras are used for capturing the variations in the droplet shapes during its ejection time to drop's breakup time. Through this technique, researchers evaluate the effect of jetting speed, nozzle size, and material properties on the dynamic of the drop formation process [7-12]. Other than experimental techniques, several computational and numerical methods are introduced for the investigation of drop detachment process. Badie and Lange [13] considered the finite element method for the simulation drop on demand droplet formation. Feng [14] applied finite volume method for the simulation of the drop formation. The numerical methods used for tracking the evolution of the droplet's free surface are a tough task especially during the breakage and merging of the drop's thread. In these methods, we have to solve both the Continuity equation and the Navier- Stokes equation; which is a complicated task.

Researchers are dealing with this subject under the banner of two-phase flows. Here, drop's formation and its breakup at a various capillary angle are quite interesting. Study of wettability basically involves the measurement of contact angles as core data, which represents the degree of wetting when a solid and liquid interact. It plays an important role in various industrial processes like liquid coating, spray painting, lubrication etc.

The degree of wettability is divided into two segments. High wettability represents when the value of contact angle is less than 90˚ and low wettability represents when the contact angle is greater than 90˚. More specifically, if the contact angle is less than 90˚, it means the surface is favorable for wetting, i.e. fluid takes a large surface area on the surface. Similarly, if the contact angle is more than 90˚, it means the surface is not favorable for wetting and the liquid will minimize its contact surface area and form a spherical droplet. The shape of the liquid drop is decided by the surface tension of the liquid. In a liquid droplet, each molecule is being pulled equally by neighboring molecules, due to which no net force develops in the droplet. At the surface of the droplet, due to unavailability of molecules, some positive net forces act, which pulls the neighboring molecules inwards. This causes the drop to be spherical in shape.

In 1805, Young [15] investigated the contact angle of a liquid drop on a solid surface by comparing the three interfacial tensions as:

$$\gamma_{lv}\cos\theta_Y = \gamma_{sv} - \gamma_{sl}$$

where γ_{lv}, γ_{sv}, γ_{sl} represents the surface tension between liquid- vapor, solid- vapor and solid-liquid phases respectively, θ_Y is Young's contact angle.

A new relationship between the drop base radius and the contact angle was developed from theoretical relationship named as modified Young's equation. Gajewski [16] confirms the hysteresis impact on the sessile drops' contact points with expanding drop diameters and diminishing diameters even on metallic surfaces. He proved that aluminum and stainless steel have zero hydrophobic properties when the diameter of the drop increases or decreases while this was not observed with copper and metal. He affirms that the basic contact angle depends upon the compound properties of the surface and on surface roughness. Lam [17] analyzed the advancing and receding of contact angles of 21 different liquid samples through automated Axisymmetric Drop Shape Analysis-

Profile (ADSA-P). Moraila – Martinez et al. [18] monitored different receding sessile drop at different static contact angle at low capillary numbers.

Recently, some experimental and numerical studies were carried out that focused on the wettability of the nozzle tip and the nozzle plate surface [19-20]. Lai et al. [21] studied the effect of contact angle during the ejection of a droplet in which the model has a vibrational motion instead of inkjet jet. For the analysis of complex fluid system having phase transition, the Lattice Boltzmann method was used for the computation work [22-27].

This paper includes the study to compute the effect of contact angle on various parameters of drop formation. The parameters include breakup thread length, breakup velocity, breakup/ detachment time through CFD by considering the Volume of Fluid method. Wettability of nozzle depends on the material property and contact angle. Contact angle varies from advanced contact angle (maximum) to receding contact angle (minimum). In this simulation work, the contact angle variation of 60˚ to 180˚ was investigated while the rate of the drop's ejection for the simulation work is considered as 0.1m/s. Different detachment profile shape of the drop is shown at regular interval of time spectrum.

2. COMPUTATIONAL SIMULATION OF CAPILLARY TUBE

2.1 Methodology

A 2D model geometry of the nozzle is constructed whose dimension is given in Figure 1. All zones of the model are defined to the system as shown in Figure 1. A laminar flow model was considered and assigned the direction of gravitational force towards the z-direction. A fully developed flow through the nozzle was assumed for the simulation, and a user-defined function of velocity flow is developed attached to the assumed model's boundary condition. Pressure Implicit with Splitting of Operators (PISO) algorithm along with PREssure STaggering Option (PRESTO) scheme was used for the discretization process. Under-relaxation factor for pressure was 0.3 and that for momentum as 0.7, was used for the convergence of all variables. The convergence of the discretized equations was said to have been achieved when the whole field residual for all the variables fell below 10^{-3} for u_x, v_y. The order of magnitude of dimensionless numbers G, Ca and Re are 4.65×10^5, 1.71×10^{-1} and 3.46×10^0 respectively.

2.2 Rheological properties

The liquid used for the simulation process was Glycerin. The physical properties of Glycerin in the air at room temperature are given in Table 1. The value of physical properties of Glycerol solution is taken from literature [28].

Table 1. Physical property of 85% Glycerin [28]

Viscosity (kg/ms)	Surface Tension (N/m)	Density (kg/m³)
0.1129	0.066	1223

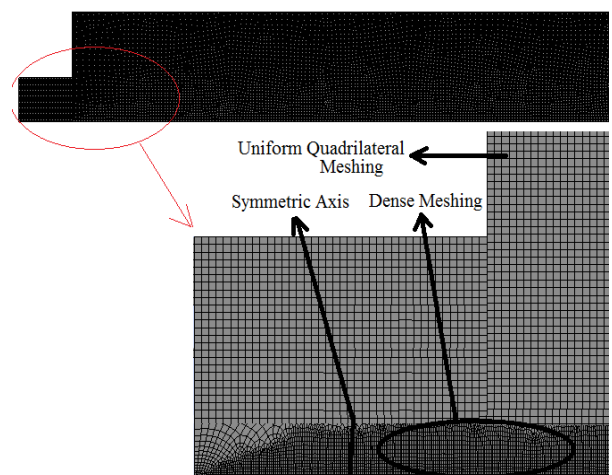## 3. COMPUTATIONAL DOMAIN AND MESH

3.1 Modeling of physical domain

Figure 1 shows the geometric model of the computational domain developed in the ANSYS-FLUENT module along with the necessary boundary conditions. The computational domain is a rectangular nozzle with the length of 30 mm and the width of 8 mm. The radius of the nozzle is 1.6 mm. The computational domain is validated with the experimental results [29] which shows that the increase in viscosity increases the thread length of the drop. It is also observed that the size of the primary drop increases slightly with the increase in surface tension and decrease in viscosity whereas the effect of density on the size of the primary drop is negligible. The green shaded region shows the Newtonian fluid named 85% Glycerin aqueous solution, whereas the grey shaded region is an air chamber.
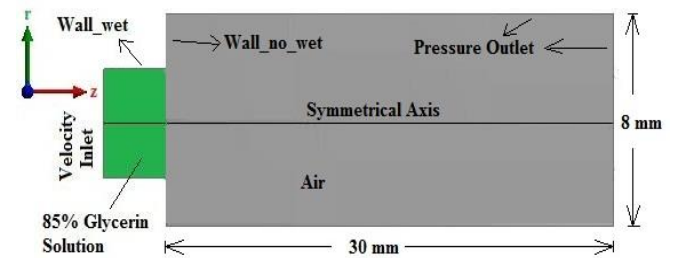
**Figure 1.** Computational physical domain

3.2 Mesh generation

Figure 2 shows the meshing of the computational domain. Meshing plays an important role in finding the numerical solutions of the physical problem through computational methods. For precise results, grid size should be small or one can say that the number of the cells must be more. The cell density near the axisymmetric axis is too dense as compared to the other zone of the computational domain. This improves the accuracy of drop generation and its transport profile. Meshed cells are quadrilateral in shape. A total of 80000 meshing cells were used for the computation process.

Figure 2. Meshing of the computational domain

3.3 Grid independence test

Grid independence test was used to determine the precision of the computational results for different meshing conditions. Figure 3 shows the profile of drop formation at 1.5ms and 3ms respectively.
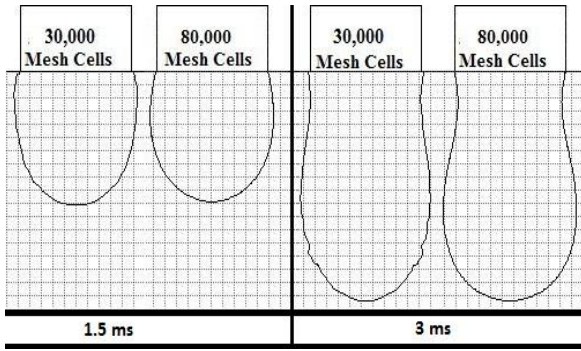
Figure 3. Grid independence test

As shown in Figure 3, the periphery of glycerol droplet in case of 30,000 meshing cells was not smooth as compared to that of 80,000 cells. Increased meshing cells not only smooth the drop's profile, but it will increase the computation time.

3.4 Boundary condition and solution parameters

To examine the drop dynamics process, 'Volume of Fluid' model was used. The volume of Fluid method was used to locate the drop's profile during its detachment process. To initiate the ejection process, a velocity user-defined function (UDF) was intercepted with the VOF model. The whole process took place under the atmospheric pressure conditions. The following assumptions were included in the process:

Assumptions:
- The computational model is axisymmetric.
- The incompressible property is considered for the surrounding air.
- The physical properties of the liquid are known and constant.
- Evaporation phenomenon for the liquid is neglected.
- At the inlet of the capillary tube, fluid flow is assumed to be fully developed flow.
- The thickness of the capillary tube exit is neglected [30].

The Boundary Condition used for the computation is marked in Figure 1 and also stated:
- Inlet of the domain is velocity inlet.
- Axis is considered as an axisymmetric axis.
- Free slip velocity condition near the wall because the fluid near the wall is air.
- The outlet of the computational domain is an atmospheric pressure outlet.

3.5 Mathematical modeling

Based on the above-mentioned assumptions, the Navier-Stokes Equation in non-dimensional form for the transient motion of the liquid is considered as,

$$\nabla . v = 0, \tag{1}$$

$$Re\left(\frac{\partial v}{\partial t} + v . \nabla v\right) = \nabla . \tau + \left(\frac{G}{Ca}\right) j \tag{2}$$

$$\tau = -pI + [\nabla v + (\nabla v)^T] \tag{3}$$

The variables in Eq. (1) are, ∇ is the gradient operator; v is the resultant velocity vector. Similarly, in Eq. (2), τ is the stress tensor; j is the unit vector in the z-direction. In Eq. (3), p represents the dimensionless pressure and I is the identity tensor.

Also during the non-dimensionalization process, three dimensionless numbers are introduced in Eq. (2),

Reynolds number, $Re = \rho UD/\rho$,
Gravitational Bond number, $G = \rho gR2/\sigma$,
Capillary number, $Ca = \mu U/\sigma$

The flow is considered as fully developed, so its velocity profile becomes,

$$v_z = \frac{2Q}{\pi R^2}\left\{1 - \left(\frac{r}{R}\right)^2\right\} \ , 0 \le r \le R \tag{4}$$

where, r is the radial coordinate of drop phase, and vz is the flow velocity in the z-direction.

The maximum velocity of liquid phase flow for the fully developed flow is given as:

$$U = \frac{2Q}{\pi R^2} \tag{5}$$

4. RESULTS AND DISCUSSION

Contact angle gives the quantitative measures of wetting of solid by a liquid. It is the angle formed by the liquid at the three-phase boundary where liquid, solid and gas intersects. Low contact angle indicates that the liquid spreads on the solid surface or it can be said that it wets the surface area. Whereas the high contact angle shows the poor spreading of a liquid on the solid surface and solid surface remains unwetted due to the liquid.

In this work, the effect of contact angle on the shape and size of the droplets generated has been investigated by keeping remaining physical parameters constant.
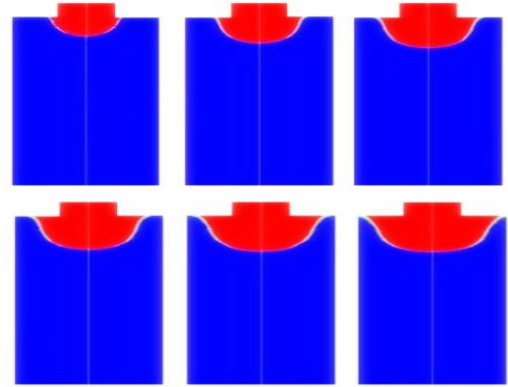

Figure 4. Drop detachment process for contact angle 60˚

Figure 4 shows the drop breakoff process of the glycerin liquid when the contact angle between the liquid and the material is 60˚. As the contact angle 60˚ is less than 90˚ it displays the high wettability of the nozzle. Due to this high wettability, glycerin liquid remains in contact with the wall of the capillary tube. As the wetting condition is favorable for the Glycerin liquid, it spreads on the nozzle wall over a large area. Figure 4 shows that owing to the high wettability condition, the thinning out tendency of the drop is not so good. It begins spreading in both downward as well as transversal sides in the domain.

As earlier described, we investigated wettability of the nozzle's inner wall as the prime parameter which plays an important role in controlling the quality of inkjet as well as spray painting.
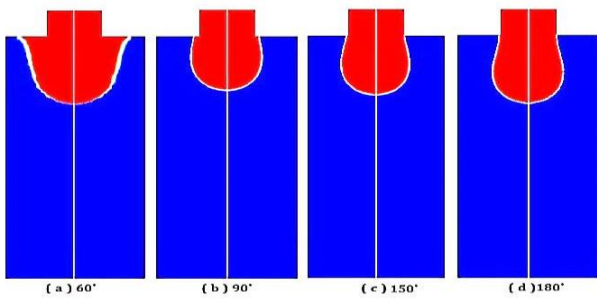
Figure 5. Droplet images at the evolution time at nozzle inner wall contact angles of (a) θ=60°, (b) θ=90°, (c) θ=150°, (d) θ=180°

Figure 5 shows the drop formation at the initial time of ejection. It can be seen that for contact angle less than 90˚, the glycerin spreads on the nozzle inline, whereas when the contact angle is more than 90˚, the motion of the glycerin liquid is more towards the vertical direction. The profile of drops during detachment for the low wettability is good and clear. The hydrophilic wall demonstrates stronger adhesion to the liquid as shown in Fig 5(a). When the contact angle increases from 90˚ to 180˚, the liquid filament before the break up become thinner and longer, it means the time to obtain the first droplet is getting increased. The long filament is the main factor that increases the probability of the satellite droplet formation. These satellite drops will reduce the quality of both spray painting in automobile sectors and inkjet printing in printing industries. Figure 6 shows the detachment profile of the flow field at the instant of droplet breakup. These contours exhibit that a more hydrophobic nozzle doesn't permit the drop's liquid to spread on the inner lining of nozzle although the thread length of the droplet extends over a greater distance.
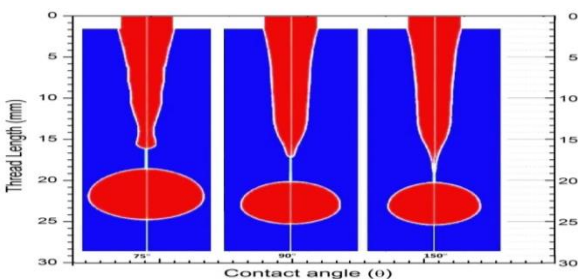
Figure 6. Droplet images at the breakup moment at nozzle inner wall contact angles of (a) θ=75°, (b) θ=90°, (c) θ=150°

For the hydrophilic nozzles, the droplet breaks up earlier and also generates a shorter and thicker filament. A hydrophilic inner wall is, therefore, a valuable design feature that can improve the print quality. Also, as shown in Figure 6, the contact angle equal to and below 75˚ leads to a quite thicker filament, which means that the volume of the droplet is more during ejection and will also reduce the print quality. Hence it is not advisable to use an extremely hydrophilic nozzle.

From Figure 7, it can be seen that the droplet breakup velocity, thread length of the drop before the breakup and its breakup time depends on the nozzle's wall wettability. At low contact angle, the fluid is hydrophilic, and it takes more time to break off at a very low velocity. As the contact angle increases from 60˚ to 180˚, the thread length and breakoff velocity increase by 12.5 % and 74% (approx.) respectively, whereas the breakoff time decreases by 70% (approx.).

5. CONCLUSIONS

Based on the computational analysis and rational discussions, the following conclusions are arrived:

(1) The comparison of the numerical results with the experimental observations is found to be in good agreement, indicating the ability of the present computational domain to simulate the drop formation.

(2) A computational model was used to investigate the role of wettability in the droplet formation. A number of simulations were performed and their result was analyzed with three important properties: the drop's thread length, the breakup velocity of the drop, and the breakup time.

(3) With increase in contact angle from 60˚ to 180˚;
- the breakup time decreased by 70% (approx.).
- the droplet velocity increased by 74% (approx.).
- the thread length increases by 12.5 %.

(4) The hydrophobic nature nozzle increases the thread length of the drop which produces the satellite drops. This results in the improved printing quality and performance.
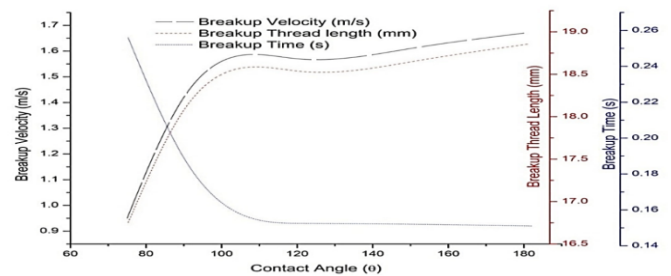
Figure 7. Variations in the breakup velocity, breakup thread length and breakup time with the changes in wettability of the nozzle inner wall

REFERENCES

[1] Liu F. (2018). Numerical analysis of droplet atomization in wet electrostatic precipitator based on computational particle-fluid dynamics. International Journal of Heat and Technology 36(1): 215-221. https://doi.org/10.18280/ijht.360129

[2] Fan JW, Liu Y, Liu LL, Yang SR. (2017). Hydrodynamics of residual oil droplet displaced by polymer solution in micro-channels of lipophilic rocks. International Journal of Heat and Technology 35(1): 611-618. https://doi.org/10.18280/ijht.350318

[3] Wijshoff H. (2010). The dynamics of the piezo inkjet printhead operation. Physics Report 491: 77-177. http://dx.doi.org/10.1016/j.physrep.2010.03.003

[4] Singh M. (2010). Inkjet printing-process and its applications. Advance Material 22: 673-685. https://doi.org/10.1002/adma.200901141

[5] Basaran OA. (2013). Nonstandard ink jets. Annual Review of Fluid Mechanics 45: 85-113. https://doi.org/10.1146/annurev-fluid-120710-101148

[6] Eggers J. (1997). Nonlinear dynamics and breakup of free surface flows. Reviews of Modern Physics 69(3): 865-929. https://doi.org/10.1103/RevModPhys.69.865

[7] van der Bos A, van der Meulen MJ, Driessen T, van den Berg M, Reinten H, Wijshoff H, Michel Versluis Lohse D. (2014). Velocity profile inside piezoacoustic inkjet droplets in flight: comparison between experiment and

numerical simulation. Physical Review Applied 1(1): 014004. https://doi.org/10.1103/PhysRevApplied.1.014004

[8] (2014). Physics: Fast imaging captures falling droplets. Nature. 507(142). http://dx.doi.org/10.1038/507142a

[9] Dong H, Carr WW. (2006). An experimental study of drop-on-demand drop formation. Physics of Fluids 18: 072102. https://doi.org/10.1063/1.2217929

[10] Kwon KS. (2009). Speed measurement of ink droplet by using edge detection techniques. Measurement 42: 44-50.
http://dx.doi.org/10.1016/j.measurement.2008.03.016

[11] Castrej´on-Pita JR. (2011). Experiments and Lagrangian simulations on the formation of droplets in drop-on-demand mode. Physical Review E 83: 036306.

[12] Castrejo´n-Pita AA. (2012). Breakup of liquid filaments. Physical Review Letters 108: 074506.

[13] Badie R, Lange DFD (1997). Canism of drop constriction in a drop-on-demand inkjet system. Proceedings of Royal Society of London A 453: 2573-2581. http://dx.doi.org/10.1098/rspa.1997.0137

[14] Feng JQ. (2002). A general fluid dynamic analysis of drop ejection in drop-on-demand ink jet devices. Journal of Imaging Science and Technology 46: 398-408.

[15] Young T. (1805). An essay on the cohesion of the fluids. Philosophical Transactions of the Royal Society of London 95: 65-87. http://dx.doi.org/10.1098/rstl.1805.0005

[16] Gajewski A. (2008). Contact angle and sessile drop diameter hysteresis on metal surfaces. International Journal of Heat Mass Transfer 51: 4628–4636. http://dx.doi.org/10.1016/j.ijheatmasstransfer.2008.01.027

[17] Lam CNC, Kim N, Hui DKDY, Kwok DY, Hair ML, Neumann AW. (2001). The effect of liquid properties to contact angle hysteresis. Colloids and Surfaces A: Physicochemical and Engineering Aspects 189(1-3): 265-278.

[18] Carmen Moraila-Martínez L. (2012). The efect of contact line dynamics and drop formation on measured values of receding contact angle at very low capillary numbers. Colloids and Surfaces A: Physicochemical Engineering Aspects 404: 63–69. https://doi.org/10.1016/j.colsurfa.2012.04.012

[19] Choi KH, Rahman A, Ko JB, Rehmani A, Ali A, Doh YH, Kim DS. (2010). Development and ejection behavior of different material-based electrostatic ink-jet heads. The International Journal of Advanced Manufacturing Technology 48(1-4): 165-173.

[20] Kim YJ, Choi J, Son SU, Lee S, Nguyen XH, Nguyen VD, Byun D, Ko HS. (2010). Comparative study on ejection phenomena of droplets from electro-hydrodynamic jet by hydrophobic and hydrophilic coatings of nozzles. Japanese Journal of Applied Physics 49(6R): 060217.

[21] Lai JM. (2010). Influence of liquid hydrophobicity and nozzle passage curvature on microfluidic dynamics in a drop ejection process. Journal of Micromechanics and Microengineering 20: 015033. https://doi.org/10.1088/0960-1317/20/1/015033

[22] Aidun CK, Clausen JR. (2010). Lattice-Boltzmann method for complex flows. Annual Review of Fluid Mechanics 42: 439-472. https://doi.org/10.1146/annurev-fluid-121108-145519

[23] Chen SY, Doolen GD. (1998). Lattice Boltzmann method for fluid flows. Annual Review of Fluid Mechanics 30: 329-364. https://doi.org/10.1146/annurev.fluid.30.1.329

[24] Ladd AJC, Verberg R. (2001). Lattice-Boltzmann simulations of particle-fluid suspensions. Journal of Statistical Physics 104: 1191-1251. https://doi.org/10.1023/A:1010414013942

[25] Zhang J. (2011). Lattice Boltzmann method for microfluidics: models and applications. Microfluid Nanofluid 10: 1-28. https://doi.org/10.1007/s10404-010-0624-1

[26] Wen B. (2015). Thermodynamic - consistent lattice Boltzmann model for non-ideal fluids. Europhysics Letter 112: 44002. https://doi.org/10.1209/0295-5075/112/44002

[27] Wen B. (2014). Galilean invariant fluid-solid interfacial dynamics in lattice Boltzmann simulations. Journal of Computational Physics 266: 161-170.

[28] Timmermans J. (1960). The physico-chemical constants of binary systems in concentrated solutions: Systems with inorganic+ organic or inorganic compounds (excepting metallic derivatives). Interscience Publishers 4.

[29] Pardeep, Srivastava M, Sinha MK. (2018). Numerical simulation of dynamics of the drop formation at a vertical capillary tube. In: Singh M., Kushvah B., Seth G., Prakash J. (eds) Applications of Fluid Dynamics. Lecture Notes in Mechanical Engineering. Springer, Singapore. https://doi.org/10.1007/978-981-10-5329-0_27

[30] Wilkes ED. (1999). Computational and experimental analysis of dynamics of drop formation. Physics of fluids 11(12): 3577-3598. https://doi.org/10.1063/1.870224

NOMENCLATURE

p	Dimensionless pressure
v	flow velocity (m/s)
VOF	Volume of Fluid model
UDF	User Defined Function

Greek symbols

γ	Surface Tension between different phases(N/m)
θ	Contact Angle (°)
∇	gradient operator
V	Resultant velocity vector
τ	stress tensor
ρ	Density of the fluid(kg/m^3)
μ	Viscosity of the fluid(kg/ms)

Subscripts

Y	Young's contact angle
lv	liquid- vapor phases
sv	solid- vapor phases
sl	solid-liquid phases
z	z-direction